# Faraday conversion as a diagnostic of Fast Radio Burst progenitors

# H. K. Vedantham, <sup>1★</sup> V. Ravi<sup>2</sup>

<sup>1</sup>ASTRON, Netherlands Institute for Radio Astronomy, Oude Hoogeveensedijk 4, 7991PD, Dwingeloo, The Netherlands

Accepted XXX. Received YYY; in original form ZZZ

#### ABSTRACT

The extreme, time-variable Faraday rotation observed in the repeating fast radio burst (FRB) 121102 demonstrates that some FRBs originate in dense and dynamic magneto-ionic environments. Here we show that besides rotation of the linear-polarisation vector (Faraday rotation), such media will generally convert linear to circular polarisation (Faraday conversion). We use the stringent constraints on circularly polarised emission in bursts from FRB 121102 to conclude the following. (i) All one-zone models where the persistent radio source associated with FRB 121102 and the Faraday rotation are generated by the same relativistic plasma are ruled out. (ii) The Faraday rotation must occur in non-relativistic plasma where the characteristic magnetic field, B, is determined to within a factor of order unity:  $10\,\mathrm{mG} \lesssim B \lesssim 30\,\mathrm{mG}$ . (iii) The value of B is close to the equipartition magnetic field of the persistent radio source associated with FRB 121102, suggesting that the Faraday rotating medium and the synchrotron-emitting plasma of the persistent source are nonetheless co-located. We apply these constraints to proposed models for persistent source and Faraday screen associated with FRB 121102.

# 1 INTRODUCTION

By virtue of their large Faraday rotation measures, at least two Fast Radio Burst (FRB) sources (FRB 121102, FRB 110523; Spitler et al. 2014; Masui et al. 2015) are observed to reside in dense magneto-ionic environments. In addition to Faraday rotation, propagation through a magnetoionic medium leads to Faraday conversion wherein linearly polarised light is converted to circularly polarised light and vice-versa (Sazonov 1969; Pacholczyk & Swihart 1970; Huang & Shcherbakov 2011). If the Faraday rotation angle (Stokes Q-U rotation) is  $\phi_{FR}$ , then in the absence of geometric factors and relativistic corrections, the Faraday conversion angle (Stokes U–V rotation) is  $\phi_{FC} = \phi_{FR} \nu_B / \nu$  where  $\nu$ is the radio-wave frequency and  $\nu_{\rm B}$  is the electron cyclotron frequency. Faraday conversion is insignificant in the Milky Way interstellar medium (ISM; where  $\nu_{\rm B} \sim 10\,{\rm Hz}$ ), and is normally disregarded in radio-polarimetric analyses. However, Faraday conversion is thought to explain the significant circular-polarisation fractions observed in Active Galactic Nuclei jets (Homan et al. 2001) and in Sgr A\* (Bower et al. 2002), where the radiation propagates through media with much larger magnetic fields than the Milky Way ISM.

In this paper, by taking FRB 121102 as a test case, we argue that Faraday conversion is an observable effect in some FRBs and leads to important limits on the magnetic

field strength in the circum-burst media. We show that additional constraints from temporal variations in the dispersion and Faraday rotation of FRB 121102 critically constrain proposed models for the environment of FRB 121102.

In §2, we summarise existing physical constraints on the magneto-ionic environment of FRB 121102 and its associated persistent radio source. In §3, we describe the additional constraints implied by the non-detection of circular polarisation in FRB 121102, given predictions from Faraday conversion. We discuss the implications of these results for models where FRB 121102 is located within the persistent radio source in §4, and conclude in §5.

# 2 OBSERVED CONSTRAINTS ON THE ENVIRONMENT OF FRB 121102

# 2.1 Observations

We first summarise the known properties of the magneto-ionic environment surrounding the repeating FRB 121102 (Spitler et al. 2016). It has been localised to an HII region in a galaxy at a redshift z=0.19 (luminosity and angular-diameter distances of  $d_{\rm L}\approx 970\,{\rm Mpc}$  and  $d_{\rm A}\approx 680\,{\rm Mpc}$  respectively; Chatterjee et al. 2017). Additionally, the FRB 121102 bursts are (i) co-located to within 40 pc (95% confidence) with a persistent flat-spectrum (1–10 GHz) radio source with flux-density  $S_{\nu}\approx 200\,\mu{\rm Jy}$  at 3 GHz (Marcote et al. 2017), and (ii) show very high levels of Faraday rotation, quantified by the rotation measure, RM =

<sup>&</sup>lt;sup>2</sup> Harvard-Smithsonian Center for Astrophysics, 60 Garden Street, Cambridge, MA 02138, USA

 $<sup>^{1}</sup>$   $v_{\rm B}=eB/(2\pi m_{e}c)$ , where e is the electron charge, B is the magnetic field strength,  $m_{e}$  is the electron mass and c is the speed of light in vacuum.

 $1.46\times10^5\,\mathrm{rad}\,\mathrm{m}^{-2}$  in the source frame. The RM reduced by  $\sim10\%$  in seven months (Michilli et al. 2018), whereas its dispersion measure increased by just  $1-3\,\mathrm{pc}\,\mathrm{cm}^{-3}$  in four years (Hessels et al. 2018).

### 2.2 Dispersion and Faraday rotation

The dispersion measure in the entire host galaxy is constrained to be less than  $250\,\mathrm{pc\,cm^{-3}}$  (Tendulkar et al. 2017). If an amount,  $\mathrm{DM_{RM}}$ , of that is in the Faraday rotating nebula, Hessels et al. (2018) obtain the following bound by requiring the magneto-ionic medium to be transparent to free-free absorption at the lowest frequency at which bursts have been observed (1 GHz):

$$T_4^{2.3} \text{DM}_{\text{RM}} > 150 \left( \frac{\beta}{\eta_R^2} \right)$$
 (1)

where  $T_4$  is the gas temperature in units of  $10^4$  K,  $\beta$  is the ratio of thermal to magnetic pressure, and  $\eta_B \leq 1$  is a geometric factor equal to the mean value of  $\cos\theta$  along the ray path in the Faraday rotating medium where  $\theta$  is the angle the ray makes with the ambient magnetic field. For an ordered field, we have  $\eta_B = \cos\theta$ . Significantly smaller values must be expected for a highly tangled field due to partial cancellation of positive and negative Faraday rotation. Further, for any given choice of  $DM_{RM}$ , the corresponding magnetic field that can generate the observed Faraday rotation is

$$B = \frac{0.18}{\text{DM}_{\text{RM}}\eta_B} \text{ G} \tag{2}$$

We now address the RM variations using two generic models for the magneto-ionic medium. We will address specific models in  $\S 4$ .

Expanding nebula: If the observed RM decrease is due to the expansion of a nebula of radius R (e.g., Waxman 2017; Margalit & Metzger 2018), then  ${\rm DM_{RM}} \propto R^{-2}$  and  $B \propto R^{-1.5}$ , maintaining the same plasma  $\beta$  and geometric factor  $\eta_B$ . We therefore have  $\Delta RM/RM = \Delta B/B + \Delta DM_{RM}/DM_{RM}$ , where (to first order)  $\Delta B/B = -1.5\Delta R/R$ , and  $\Delta {\rm DM_{RM}}/{\rm DM_{RM}} =$  $-2\Delta R/R$ . The observed 10% variation in RM over seven months then implies  $\Delta R/R \approx 0.05 \,\mathrm{yr}^{-1}$  and the nebula is therefore expanding on a timescale of about  $\tau \approx 20$  years. The implied -5.8% decrease in DM<sub>RM</sub> due to the expansion must be insignificant compared to the observed increase of  $1 - 3 \,\mathrm{pc}\,\mathrm{cm}^{-3}$  in the total DM over a longer timescale than the reported RM variations; the observed DM variations presumably occur in plasma unrelated to the Faradayrotating plasma. Hence we can safely place the constraint  $DM_{RM} < 17.5 \,\mathrm{pc}\,\mathrm{cm}^{-3}$ . These constraints do not differ significantly for other expansion scenarios. For instance, adiabatic expansion of a tangled field  $(B \propto R^{-2})$ , gives  $\tau \approx 23.33$  yr and  $DM_{RM} < 20 \, pc \, cm^{-3}$ 

Transverse motion: Alternatively, the RM variations could be due to transverse motion of the FRB source across a nebula over a characteristic timescale of  $\tau\approx5.83\,\mathrm{yr}.$  Let the line-of-sight extent of the Faraday-rotating nebula be equal to its transverse scale length. Then we have  $\Delta RM/RM\approx\Delta DM_{RM}/DM_{RM}\approx0.1.$  The lack of significant DM variations accompanying the RM variations now gives a more stringent constraint of  $DM_{RM}<10\,\mathrm{pc}\,\mathrm{cm}^{-3}.$ 

Using the formalism from §4.4 of Hessels et al. (2018),

we can translate the above limits on  $DM_{RM}$  to the underlying plasma parameters ( $DM_{10} = DM_{RM}/(10\,\mathrm{pc\,cm^{-3}})$  hereafter):

$$DM_{10} < (1.75, 1.0)$$

$$T_4 > 2.72 \left(\frac{\beta}{\eta_B^2}\right)^{1/2.3} DM_{10}^{1/2.3}$$

$$B = 18/(DM_{10}\eta_B) \text{ mG}$$

$$n_e = 9.3 \times 10^6 \left(\frac{\eta_B^2 T_4}{\beta}\right)^{-1} DM_{10}^{-2} \text{ cm}^{-3}$$

$$l = 1.1 \times 10^{-6} \left(\frac{\eta_B^2 T_4}{\beta}\right) DM_{10}^3 \text{ pc}$$

$$\tau = (20, 5.83) \text{ yr}$$

$$v = (0.054, 0.185) \left(\frac{\eta_B^2 T_4}{\beta}\right) DM_{10}^3 \text{ km s}^{-1}$$
 (3

Here the two limits within parentheses are for the expandingnebula and transverse-motion scenarios respectively, and l and  $n_e$  are the thickness and electron density of the Faradayrotating medium respectively. The velocities in the two cases are interpreted as the radial expansion speed of the nebula and transverse speed of the source with respect to the Faraday rotating medium, respectively. We will return to these constrains with regards to specific models in  $\S 4$ .

# 2.3 The persistent radio source

The properties of the persistent radio source associated with FRB 121102 may be constrained independently of the Faraday-rotating medium. We assume equipartition between the relativistic gas and magnetic field as is common in synchrotron sources<sup>2</sup> (Readhead 1994). The source becomes self-absorbed at  $1.5\,\mathrm{GHz}$  for radius  $R_\mathrm{per} < 0.05\,\mathrm{pc};$  this is thus the lower bound on the source size. European VLBI Network observations of the source at 5 GHz set an upper bound on the source size of  $R_{\rm per}\lesssim 1\,{\rm pc}$  (Marcote et al. 2017). This is consistent with the  $\approx 30\%$  amplitude modulations observed in the source at 3 GHz (Chatterjee et al. 2017) being caused by refractive interstellar scintillation in the Milky Way ISM (Walker 1998). For any radius within the allowed range (0.05  $< R_{per}/pc < 1$ ), we can determine the equipartition magnetic field,  $B_{eq}$ , and the column of relativistic electrons,  $N_{\rm rel}$ , using the standard expressions for synchrotron emissivity and absorption coefficients (Rybicki & Lightman 1979, their eqns. 6.36 & 6.53). We assume a powerlaw energy distribution of radiating electrons with index b = -2.5 extending between Lorentz factors  $\gamma_{\min}$  and  $\gamma_{\max}$ that are chosen to yield emission at 1 and 10 GHz respectively. The equipartition magnetic field and electron column thus determined for minimum and maximum source sizes are:  $B_{\rm eq} \approx 70 \, {\rm mG}$ ,  $\gamma_{\rm min} \approx 71$ ,  $\gamma_{\rm max} \approx 230$ ,  $N_{\rm rel} \approx 0.1 \, {\rm pc \, cm^{-3}}$  for  $R_{\rm per} = 0.05 \, {\rm pc}$ , and  $B_{\rm eq} \approx 5 \, {\rm mG}$ ,  $\gamma_{\rm min} \approx 270$ ,  $\gamma_{\rm max} \approx 850$ ,  $N_{\rm rel} \approx$  $2.8 \times 10^{-3} \,\mathrm{pc}\,\mathrm{cm}^{-3}$  for  $R_{\mathrm{per}} = 1\,\mathrm{pc}$ . The reader can scale the equipartition field to other source sizes using  $B_{\rm eq}(R) \propto R^{-6/7}$ . The total energy contained in the relativistic electrons and

 $<sup>^2</sup>$  In the model of Waxman (2017), which we discuss in §4.1, equipartition is required by dynamical and source-size (from scintillation) constraints.

the magnetic field ('equipartition energy'), is  $\sim 10^{48.8}$  and  $\sim 10^{50.4}$  erg respectively. If the relativistic electrons were injected in a one-off event, the synchrotron cooling rates at  $\gamma_{\rm max}$  yield source ages of 14 yr for  $R=0.05\,{\rm pc}$  and 760 yr for  $R=1\,{\rm pc}$ . The corresponding expansion velocities are  $0.011\,c$  and  $0.0043\,c$  respectively.

#### 3 FARADAY CONVERSION LIMITS

# 3.1 Cold plasma

In non-relativistic plasma, the phase angle associated with Stokes U-V rotation due to Faraday conversion is a factor of  $(\nu_B/\nu)(1-\eta_B^2)$  lower than the Faraday rotation angle. At its peak observed RM, the latter quantity for FRB 121102 was 821.25 rad at 4 GHz. The bursts were  $\approx 100\%$  linearly polarised with the circular-polarisation fraction limited to be below about 2% (Michilli et al. 2018; Hessels et al. 2018). This requires  $(1-\eta_B^2)\nu_B/(4\,\mathrm{GHz}) < 2.4\times10^{-5}$ , which puts an upper limit on the magnetic field of  $B<34.8/(1-\eta_B^2)\,\mathrm{mG}$ , and by virtue of eqn. 2, a new lower limit on the dispersion measure of  $\mathrm{DM}_{10}>0.52(1-\eta_B^2)/\eta_B$ . Combining this with eqn. 3, we bound the magnetic field and the dispersion measure in the Faraday-rotating medium to within a factor of order unity (barring a specific geometry where  $\eta_B\approx1$ ):

$$\left(\frac{10.3}{\eta_B}, \frac{18}{\eta_B}\right) < \frac{B}{\text{mG}} < \frac{34.8}{1 - \eta_B^2}; \ \eta_B \le 1$$

$$(17.5, 10) > \frac{\text{DM}}{\text{pc cm}^{-3}} > 5.2 \frac{1 - \eta_B^2}{\eta_B} \tag{4}$$

We stress that this constraint is independent of the properties of the persistent radio source, as we have not (yet) assumed that the FRB originates from within the persistent source.

# 3.2 Hot plasma

If the FRB progenitor resides within the persistent source, then relativistically corrections must be considered to derive the levels of Faraday conversion in the persistent source. We use the approximate expressions of Huang & Shcherbakov (2011, their eqns. 51, 58 & 59), who find that Faraday conversion is stronger by almost two orders of magnitude in trans-relativistic plasma (electron Lorentz factors  $\gamma \sim$ 10 – 100). Both Faraday rotation and conversion decline for much larger values of  $\gamma$  and propagation resorts to vacuumlike conditions in ultra-relativistic gas. In Fig. 1, we plot the level of Faraday conversion in trans-relativistic gas for two commonly encountered electron distributions: a relativistic Maxwellian and a power law with an assumed index b = -2.5. The upper panels show the total rotation and conversion angles, and the lower panels show their ratios. The plots assume  $\theta = \pi/4$  (giving  $\eta_B \approx 0.707$ ), and are normalised to a total electron column of  $10 \, pc \, cm^{-3}$ .

If FRB 121102 originates from within the persistent radio source, Fig. 1 shows that the synchrotron-emitting plasma cannot also cause the observed levels of Faraday rotation of the bursts. This is seen in the bottom panels, where the rotation to conversion ratio is well above the observational upper limit (dashed horizontal line) for all relevant

electron temperature and magnetic field values determined in §2.2 and §2.3. We therefore conclude that the Faraday rotating plasma must be a distinct 'cold' population. This result is in tension with 'one-zone' models for the system (e.g., Margalit & Metzger 2018).

The relativistic electrons in the persistent source will nevertheless cause some (low) level of Faraday conversion. A model where the radio bursts propagate through the persistent source must ensure that the equipartition parameters from §2.3 do not contradict observed limits on Faraday conversion. For our edge case of  $R=0.05\,\mathrm{pc}$ ,  $B_{\mathrm{eq}}=71\,\mathrm{mG}$ ,  $\gamma_{\mathrm{min}}=70$ ,  $N_{\mathrm{rel}}=0.1\,\mathrm{pc}\,\mathrm{cm}^{-3}$ , we compute a conversion angle of 0.017 rad which is marginally consistent with observational limit of < 2%. The expected conversion fraction declines rapidly for larger source sizes bringing the equipartition model for the persistent source well within observed constraints.

#### 4 DISCUSSION

Before discussing the implications of Faraday conversion for specific models, we pause to make two observations. (i) The magnetic field in the Faraday rotating medium is constrained to the same range as that required in the persistent source based on equipartition arguments. (ii) Because Faraday conversion scales as  $v^{-3}$ , the lower limit on the field of about  $10\,\mathrm{mG}$  (eqn. 3) will result in a  $\sim 10\%$  circular-polarisation fraction at  $v \lesssim 1.3\,\mathrm{GHz}$ . It appears that the observations at 4-6 GHz were co-incidentally just beyond the 'threshold of discovery' of Faraday conversion in FRBs. We do not have more to say regarding this point save the obvious advocacy for polarimetry of radio bursts from FRB 121102 at L- and S-bands. However, point (i) may imply that the persistent source and the Faraday screen are co-located, if one rejects yet another unpalatable co-incidence as the cause. In light of this, we discuss implications for two models that explicitly make this association.

# 4.1 Expanding relativistic nebula

We first consider the generic expanding-nebula model of Waxman (2017), where the source of FRB 121102 is a compact object centrally located in a synchrotron nebula. The synchrotron nebula is confined against its tendency to relativistically expand by a much denser cold nebula. The Faraday rotation is provided by the shocked (and heated) part of the confining dense nebula. Notwithstanding the FRB generating mechanism and the nature of the compact object, this model links the velocity of the shock driven by the expanding synchrotron nebula into the surrounding colder medium and the density of the latter medium via:  $v_{\rm sh} \approx \sqrt{P_{\rm sh}/(nm_p)}$ , where  $m_p$  is the proton mass, and  $P_{\rm sh} = B^2(1+\beta)/(8\pi)$  is the pressure in the shocked part of the nebula which is similar to that in the synchrotron source. In convenient units, we have

$$v_{\rm sh} \approx 9.1 \left( \frac{T_4 (1+\beta)}{\beta} \right)^{1/2} \, \, \text{km s}^{-1}.$$
 (5)

We now equate  $v_{\rm sh}$  with the expansion velocity in eqn. 3 to obtain the following family of models for the Faraday screen:

$$T_4 = 2.94 \times 10^4 \, \beta (1+\beta) \, \eta_B^{-4} \, \text{DM}_{10}^{-6}$$

$$l = 0.0323 \, \text{DM}_{10}^{-3} \, \eta_B^{-2} \, (1+\beta) \, \text{pc}$$

$$n_e = 316.3 \, \text{DM}_{10}^4 \, \eta_B^2 \, (1+\beta)^{-1}$$

$$E_{\text{sh}} = 10^{49.2} \, \left( R_{\text{per}} / \text{pc} \right)^2 \, \text{DM}_{10}^{-5} \, \eta_B^{-4} \, (1+\beta)^2 \, \text{ergs}, \quad (6)$$

where  $E_{\rm sh}$  is the combined thermal and magnetic energy in the shock-heated Faraday screen. A feasible model from the above family must additionally satisfy the following constraints. (i) To avoid violating Faraday conversion constraints, we need  $T_4 < 10^5 \,\mathrm{K}$  (see Fig. 1 bottomleft panel). (ii) The Faraday-rotating plasma is presumably shock heated by the expanding relativistic gas, which requires the total energy in the latter to be larger than that in the former. (iii) As in Waxman (2017), we assume that the thickness of the Faraday screen must be smaller than the radius of the persistent source. The constraints on the family of models are graphically shown in Fig. 2 for a benchmark value of  $R_{\rm per}=0.5\,{\rm pc}$  and  $\beta=1.$  We find feasible parameters ranges of  ${\rm DM_{10}}\gtrsim 1.0$  and  $\eta_B\gtrsim 0.4$  with a very weak dependence on  $R_{\rm per}$ . Taken together with the constraint of  $DM_{10} < 1.75$  from  $\S 2.2,$  the allowed parameter ranges for the Faraday screen are tightly constrained:  $DM_{10} \in [1.0, 1.75]$ ,  $\eta_B \gtrsim 0.4, B\eta_B \in [10, 18] \,\mathrm{mG}, \text{ and } \log_{10}(T/\mathrm{K}) \in [7.5, 9]. \text{ It is}$ noteworthy and non-trivial that these self-consistent solutions exist after a relationship between  $\nu$ ,  $T_4$  and  $\beta$  due to eqn. 5 was imposed on observational constraints from eqn. 3.

# 4.2 Dense filaments à-la Crab

Following the suggestion by Cordes et al. (2017) that FRB 121102 is lensed by dense plasma structures similar to the cold filaments in the Crab nebula (Backer et al. 2000), we consider a model where the variable RM and DM are obtained by transverse passage of dense filaments across the line of sight to the FRB source. Hessels et al. (2018, their §4.4 & eqns. 6 to 9) have summarised the resulting constraints in terms of the peak frequency at which lensing is apparent ( $\gamma_1 = 8 \, \text{GHz}$ ), the source–lens distance  $D_{\text{sl}}$  (units of pc), and the observer–lens distance  $D_{\text{ol}} \approx D_{\text{A}} = 622 \, \text{Mpc}$ . Requiring the filament to have the same transverse and line-of-sight extents, and to be transparent to free-free absorption at 1 GHz, we obtain the following:

$$T_{4} > 5.5 \,\mathrm{DM}_{10}^{1.15} \,D_{\mathrm{sl}}^{-0.385}$$

$$n_{e} > 2.7 \times 10^{6} \,\left(\frac{\mathrm{DM}_{10}}{D_{\mathrm{sl}}}\right)^{1/2} \,\mathrm{cm}^{-3}$$

$$\left(\frac{\eta_{B} T_{4}}{\beta}\right) > 1.7 \,D_{\mathrm{sl}}^{1/2} \,\mathrm{DM}_{10}^{-2.5}$$

$$l < 3.7 \times 10^{-6} \,\left(D_{\mathrm{sl}} \mathrm{DM}_{10}\right)^{1/2} \,\mathrm{pc} \qquad (7)$$

Anticipating large electron densities for filaments located within the persistent nebula ( $d_{\rm sl} < 1$ ), we impose an additional constraint: the Bremsstrahlung-cooling timescale should exceed 10 yr. Using Rybicki & Lightman (1979, their eqn. 5.15b) the cooling-timescale is

$$\tau_{ff} = 0.26 T_4^{1/2} \left( \frac{n_e}{10^6 \,\mathrm{cm}^{-3}} \right)^{-1} \,\mathrm{yr} > 10$$
 (8)

The simplest model we consider here is one where the Faraday rotation and lensing happens in the same filamentary structure/complex. To achieve this, we need plasma parameters that satisfy eqns. 3, 7 and 8 simultaneously. A scan through the parameter space shows that self-consistent solutions are only obtained for  $\eta_B < 0.1$ . If we further require the putative filament to lie within the synchrotron nebula ( $d_{\rm ls} < 1\,{\rm pc}$ , as defined by the persistent source), then  $\eta_B \lesssim 10^{-4}$ . Even the milder constraint of  $\eta_B < 0.1$  will severely violate the bounds on the magnetic field from Faraday conversion (see eqn. 4). We therefor conclude that the same filamentary complex cannot provide the postulated plasma-lensing, and the observed Faraday rotation and variations thereof.

One could decouple Faraday-rotating and lensing plasma and readily find self-consistent solutions for two different plasma structures using eqns. 3 and 7 separately. For instance, lensing can be caused by structures with plasma parameters of  $T_4 \sim 10^5$ ,  ${\rm DM_{10}} \sim 1$ ,  $n_e \sim 10^6\,{\rm cm^{-3}}$ . The RM variations can be provided by transverse velocity of  $\sim 30\,{\rm km/s}$  across a plasma structure with parameters of  $T_4 \sim 10^2$ ,  $l \sim 2 \times 10^{-4}\,{\rm pc}$  and  $n_e \sim 5 \times 10^4\,{\rm cm^{-3}}$ .

#### 5 CONCLUSIONS

We have shown that Faraday conversion of linear to circular polarised radiation is a relevant effect for Fast Radio Bursts that propagate through dense magneto-ionic media. For our test case of FRB 121102, we conclude the following.

- (i) The lack of observed Faraday conversion at 4 GHz in FRB 121102 places an upper limit of about  $B < 30(1-\eta_B^2)^{-1}$  mG on the magnetic field in the Faraday rotating region, whereas the observed DM and RM variations place a lower limit of about  $B > 10/\eta_B$  mG ( $\eta_B \le 1$  is a geometric factor). The allowed range of B in the Faraday screen is close to the equipartition field of the synchrotron source,  $B_{\rm eq} \approx 11.5 \, (R_{\rm per}/{\rm pc})^{-6/7}$  mG suggesting that the Faraday screen and the synchrotron plasma are co-located.
- (ii) Even if the observed-frame RM of FRB 121102 has now drastically dropped to  $5\times10^4\,\mathrm{rad\,m^{-2}}$ , the lower limit of  $B=10/\eta_B\,\mathrm{mG}$  will lead to a  $\gtrsim10\%$  conversion of linearly polarised emission to Stokes V at 1 GHz at the present time (barring contrived geometries where  $\eta_B\approx1$ ). Such observations will provide a unique measurement of the magnetic field in the dense magneto-ionic medium near FRB 121102.
- (iii) The existing non-detection of circular polarisation rules out all one-zone models for FRB 121102 where the Faraday rotation and synchrotron emission are obtained from the same electron population.
- (iv) In models where the persistent source associated with FRB 121102 is confined by a colder Faraday-rotating plasma shell (for e.g. Waxman 2017), the latter is required to be shock-heated to  $\sim 10^{7.5}-10^9~\rm K$ , have an electron column of  $10-17.5~\rm pc~cm^{-3}$ , and a geometric parameter of  $0.4\lesssim\eta_B\leq1$ . The existence of such a self-consistent and over-constrained solution is not trivial and lends credence to the model. In addition to the predicted Stokes-V signal around  $\sim 1~\rm GHz$  (see (ii) above), a second strong prediction of this model is a continued downward trend in the rotation measure (with possible variations due to inhomogenities).

(v) In models involving dense filaments as in the Crab nebula, the magneto-ionic variations (DM and RM) cannot come from the same plasma structures that also act as a plasma lens which is postulated to generate certain time-frequency structures seen in FRB 121102 (Cordes et al. 2017).

We emphasise that observations targeting the detection of Faraday-converted circular polarisation at  $\sim 1\,\mathrm{GHz}$  in bursts from FRB 121102 are likely of great interest. We further advocate for 'de-rotation' circular polarised signals in FRBs with linear polarisation fractions below unity, in the event that Faraday-converted circular polarisation (with a U-V rotation angle that scales as  $v^{-3}$ ) has been averaged out. Finally, we anticipate that the arguments presented here will be of significance to other FRBs (particularly of a repeating nature) that are associated with radio-synchrotron sources and/or dense magneto-ionic media.

#### ACKNOWLEDGEMENTS

The authors thank (i) Andrei Grizinov and Eli Waxman for discussions on the implications of Faraday conversion, (ii) Eli Waxman for commenting on the manuscript, (iii) Jason Hessels for discussions regarding observational aspects of FRB 121102, and (iv) the organisers of the 2018 Schwartz/Reisman Institute for Theoretical Physics workshop on Fast Radio Bursts for their hospitality. Numerical computations used scipy, numpy, Python2.7, Python3.0 and matplotlib was used to render figures.

# REFERENCES

Masui, K., Lin, H.-H., Sievers, J., et al. 2015, Nature, 528, 523
Spitler, L. G., Cordes, J. M., Hessels, J. W. T., et al. 2014, ApJ, 790, 101

Homan, D. C., Attridge, J. M., & Wardle, J. F. C. 2001, ApJ, 556, 113

Margalit, B., & Metzger, B. D. 2018, ApJ, 868, L4

Bower, G. C., Falcke, H., Sault, R. J., & Backer, D. C. 2002, ApJ, 571, 843

Spitler, L. G., Scholz, P., Hessels, J. W. T., et al. 2016, Nature, 531, 202

Michilli, D., Seymour, A., Hessels, J. W. T., et al. 2018, Nature, 553, 182

Hessels, J. W. T., Spitler, L. G., Seymour, A. D., et al. 2018, arXiv:1811.10748

Tendulkar, S. P., Bassa, C. G., Cordes, J. M., et al. 2017, ApJ, 834, L7

Chatterjee, S., Law, C. J., Wharton, R. S., et al. 2017, Nature, 541, 58

Rybicki, G. B., & Lightman, A. P. 1979, New York, Wiley-Interscience, 1979. 393 p.,

Walker, M. A. 1998, MNRAS, 294, 307

Marcote, B., Paragi, Z., Hessels, J. W. T., et al. 2017, ApJ, 834, L8

Gajjar, V., Siemion, A. P. V., Price, D. C., et al. 2018, ApJ, 863,  $^{2}$ 

Huang, L., & Shcherbakov, R. V. 2011, MNRAS, 416, 2574

Waxman, E. 2017, ApJ, 842, 34

Cordes, J. M., Wasserman, I., Hessels, J. W. T., et al. 2017, ApJ, 842, 35

Backer, D. C., Wong, T., & Valanju, J. 2000, ApJ, 543, 740

Lorimer, D. R., Bailes, M., McLaughlin, M. A., Narkevic, D. J., & Crawford, F. 2007, Science, 318, 777

Thornton, D., Stappers, B., Bailes, M., et al. 2013, Science, 341, 53

Sazonov, V. N. 1969, Soviet Ast., 13, 396

Pacholczyk, A. G., & Swihart, T. L. 1970, ApJ, 161, 415

Readhead, A. C. S. 1994, ApJ, 426, 51

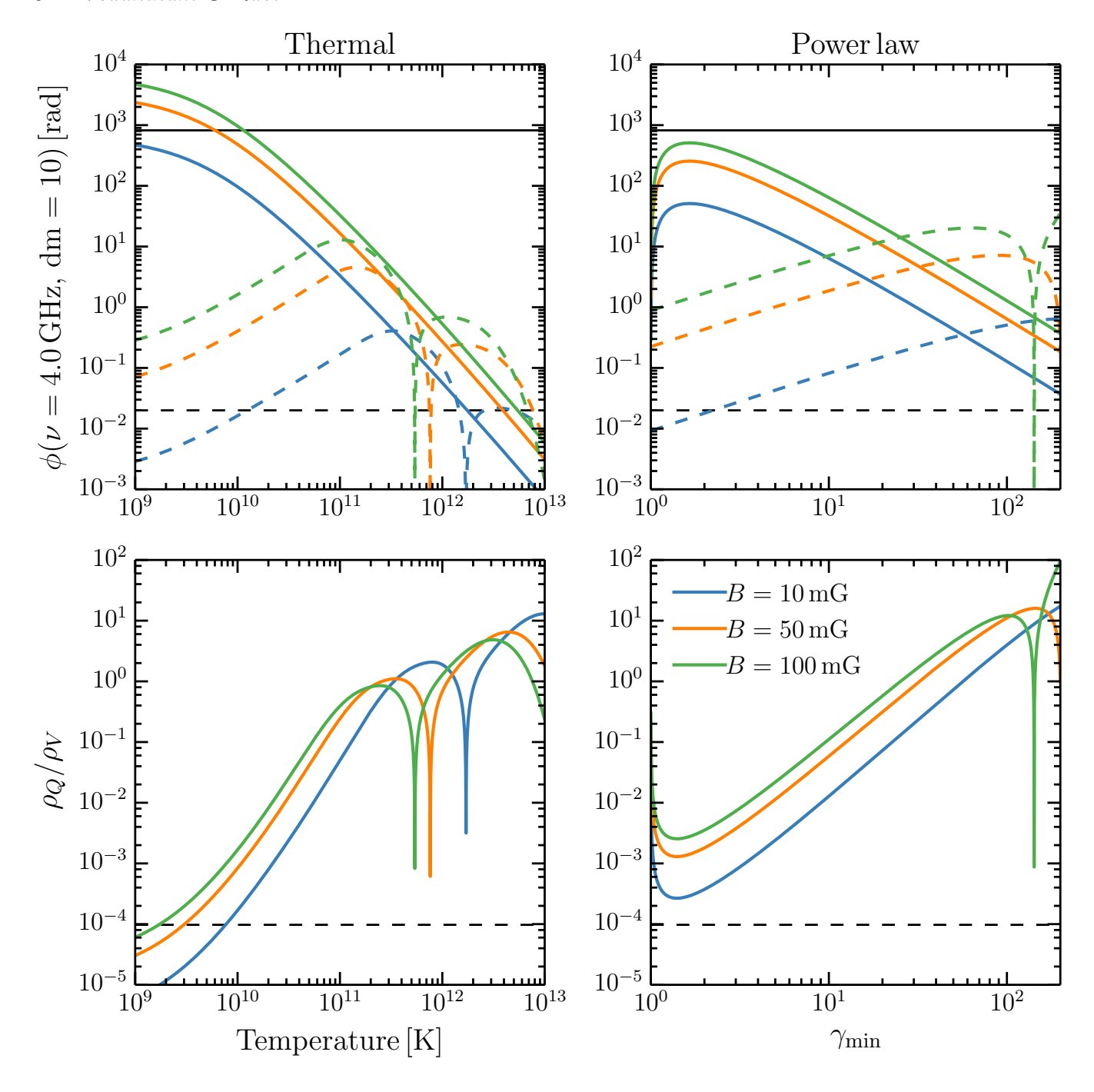


Figure 1. Faraday rotation (Q-U) and Faraday conversion (U-V) angles at  $\nu=4\,\mathrm{GHz}$  for thermal (left panels) and power law electron populations (right panels), for three different magnetic field values (different line colours). Top panels show the Faraday rotation and conversion angles (solid and dashed lines respectively). Bottom panels show the ratio of Faraday conversion angle to the Faraday rotation angle. An electron column of  $N_e=10\,\mathrm{pc\,cm^{-3}}$  (which is 10 DM units) has been assumed in all plots. The Faraday rotation angle scales as  $\phi_{Q-U} \propto BN_e v^{-2}$ . The Faraday conversion angle scales as  $\phi_{U-V} \propto B^2N_e v^{-3}$ . Dashed black line in the top panel shows the observed Faraday rotation angle  $\phi_{Q-u}$  in FRB 121102 at 4 GHz for the measured source-frame rotation measure of  $1.46 \times 10^5\,\mathrm{rad\,m^{-2}}$  (Michilli et al. 2018). The dashed black line in the bottom panels shows an upper limit on the Faraday conversion to rotation angle ratio set by the observed non-detection of conversion to Stokes V in FRB 121102. Deep notches in the Faraday conversion curves are due to zero-crossings.

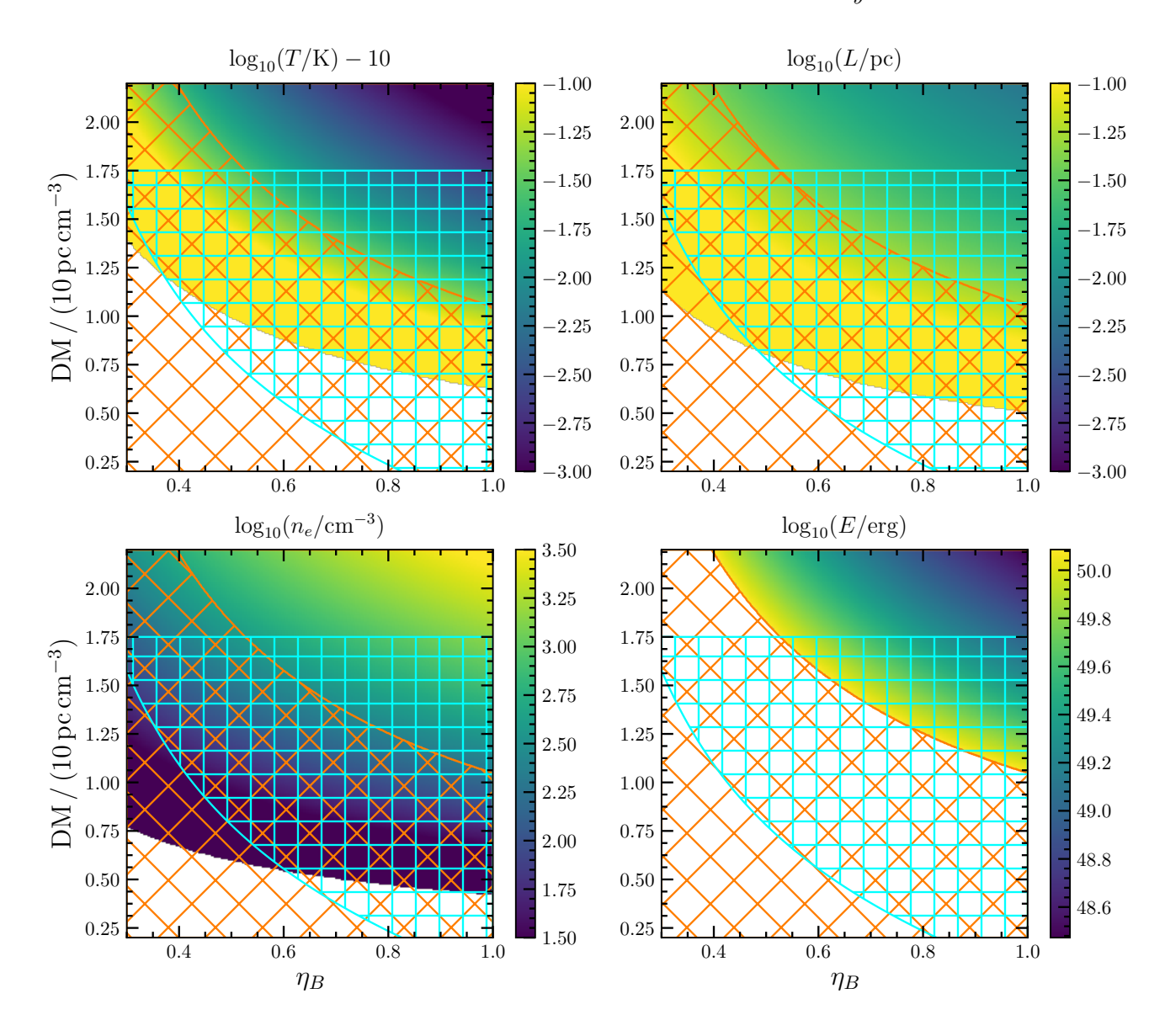


Figure 2. Constraints on the expanding nebula model of Waxman (2017) determined from eqn.6, for plasma  $\beta = 1$  and persistent source radius of  $R_{\text{per}} = 0.5$ . The cross-hatched parameter space (orange) is excluded primarily due to energetic considerations (See §4). The straight-hatched region (cyan) is the allowed parameter range due to constraints from Faraday conversion and magneto-ionic variations (see §3)